STUDY OF DIFFERENT UNMIXING ALGORITHMS IN HYPERSPECTRAL IMAGES

[1]Anjusha P V, [2]Nishanth Augustine
[1]Dept. of ECE,LBSCK
anjushakorom@gmail.com
[2]A. P.Dept. of ECE,LBSCK
Nishanthaugustine@gmail.com

Abstract-To support high level analysis of hyperspectral imagery, spectral unmixing has been used in recent years. Still, there is apresence of unavoidable spectral variability in the unmixing process, which make it difficult to accurately estimate endmembers and abundance maps in spectral unmixing. In this paper, study of different unmixing algorithms in hyperspectral images is proposed. Linear mixing model is the simplest mixing model used in hyperspectral analysis, but this model not address the spectral variations and spectral correlation. To this end, extended linear mixing model and tensor based unmixing model using low-rank strategy is proposed, which performs robustly against spectral variability problems of hyperspectral unmixing. By projecting the original data into a low-rank subspace, it can effectively reduce computational complexity in unmixing process. Furthermore, alternating direction method of multipliers-based algorithm can be used to solve the optimization problem. Experiments on synthetic and real datasets are performed to demonstrate the effectiveness and superiorityof various methods.

Index Terms —Hyperspectral data analysis, Subspace unmixing, Spectral variability,Alternating direction method of multipliers,Low-rank, Remote sensing.

I. INTRODUCTION

Hyperspectral imaging(HSI), like other spectral imaging, which analyse wide spectrum of light across the electromagnetic spectrum. HSI is a technique that uses hundreds of bands for acquiring an imageinstead of using just three primary colours (red, green, blue). HSI isorganized in the form of Data cube (3d data).An hyperspectral camera covers visible, near IR and shortwave IR region in electromagnetic spectrum. It is characterized by very rich spectral information and low spatial resolution, which help us to detect targets of interest and identify unknown materials more easily.Hyperspectral data processing and analysis, include dimensionality reduction [1], [2], image segmentation [3], land-cover detection and land-use classification [4], and target detection [5]. However,pixels in HSI suffer from the effect of spectral mixing due to a lower spatial-resolution. These material mixtures unavoidably degrade the spectrally discriminative ability, particularly in some high-level applications. Due to large number of spectral band and hence large data size, HSI processing iscomputationally complex.Unmixing reduces the data size considerably.Hyperspectral unmixing is process of decomposing the hyperspectral image into a number ofendmembers and their fractional abundances.Pure spectral components in an image is called as endmembers. The fraction occupied by the endmembers are called abundances.

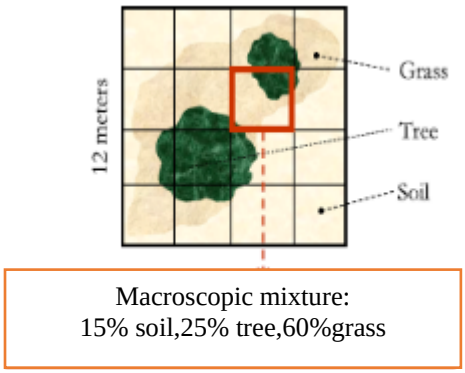

Fig 1: Endmembers and abundances present in a pixel

Figure1 illustrate the endmembers and abundances present in a pixel. Here the endmembers are tree grass and soil. Abundances are 15%,25% and 60%. The pixel contains 15% soil,25% tree and 60% grass.Spatial resolution of HSI is less as compared to other images, that means spatial portion occupied by a substance is smaller than the ground pixel size (tens of meters). As a result, the signal read by the sensor from a given spatial element of resolution and at a given spectral band is a mix of components originated from the constituent substances(endmembers), the located at that element of resolution. In this situation, the scattered energy is a mix of the endmember spectrum.

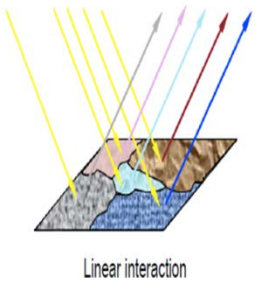

Fig 2.1. Linear interaction model

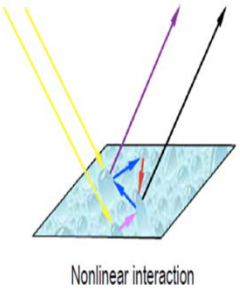

Fig 2.2. Nonlinear interaction model

The observed mixture is classified based on the mixing scale at each pixel.These areeither linear or nonlinear. The linear mixing model figure. 2.1 holds approximately when the mixing scale is macroscopic and there is negligible interaction among distinct endmembers. The nonlinear model [6] holds when the mixing scale is microscopic (i.e. intimate mixtures). Fig. 2.2 illustrates an intimate mixture, yielding a nonlinear scenario. The linear model [7] assumes negligible interaction among distinct endmembers. The nonlinear model is a complex model as compared to linear, here weassume that incident solar radiation is scattered by the scene through multiple reflection involving several endmembers. Very often, the effects of multiple scattering are assumed to be negligible and thus the linear model is adopted.

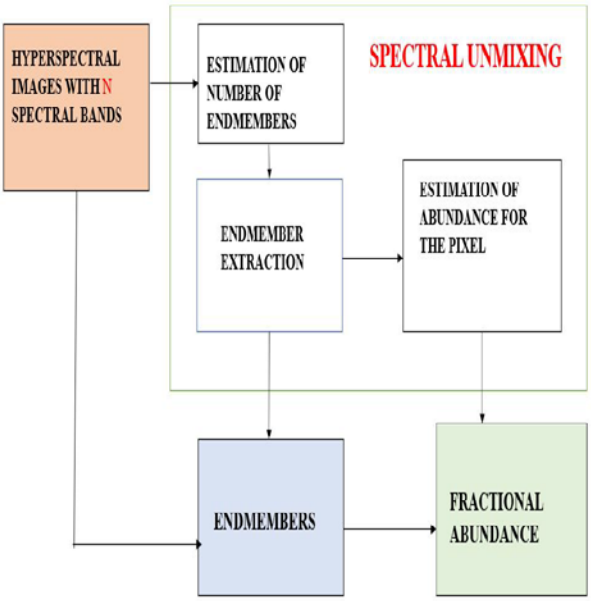

Fig 3. Block diagram of unmixing

Block diagram of unmixing is shown in figure3. The hyperspectral image with N spectral bands are input for unmixing process. In this process, first step is to estimate the number of endmembers. In second step,identified endmembers are extracted and estimate the fractional abundances. After unmixing process the endmembers and fractional abundances are obtained.

In remote sensing, spectral unmixing [8] is having many applications and the techniques have been widely and successfully applied to a variety of tasks, including mineral exploration and identification [9], forest monitoring [10],[11].Illumination and atmospheric effects are the most common cause of unmixing. Hence the radiance acquired by hyperspectral sensors cannot be directly compared with a digital spectral library or even with other radiance data sets. This comparison is made possible by the atmospheric correction, which transforms the radiance spectra into reflectance. This operation accounts for solar spectrum, sensor and sun

directions, path radiance, secondary illumination and shadowing. The second operation, data reduction, here data is reduced based of the fact that the number of endmembers present in the scene is usually much smaller than the number of bands of a hyperspectral data set. This operation has a great impact since it reduces theamount of dataas well as computational complexity, and it improves the signal-to-noise ratio (SNR). The third operation, spectral unmixing, consist of two steps: endmember determination and inversion. The first step estimates the signatures of the different endmembers present in the scene. The second step estimates the abundance [12] fractions of each endmember. To conduct the hyperspectral unmixing operation, a mixture model must be adopted to describe how the constituent endmembers and how the atmosphere scatters the sun light at a given pixel.

Assuming the absent of multiple scattering, and mixing between the materials are negligible, then the spectrum of each pixel in the HSI scene is approximately measured by a linear mixing model (LMM) [8].LMM is the simplest model used in unmixing but which does not consider the spectral variability. Without considering spectral variability, propagating unpredictable errors through LMM. To solve this issue an extended LMM (ELMM)[13],[14] was introduced. Which modelling bymultiplying different scaling factors on each endmember matrix, but is a significant shortcoming in that many spectral variabilities are not be involved correspondingly. Perturbated linear mixing model (PLMM) [15] attempts to describe the spectral variability as an additive perturbation information. Nonnegative matrix factorization (NMF) [16]ensures nonnegativity and no assumption for the presence of pure pixels. In these methods not consider the spectral variability and spectral correlation. Using a tensor based low rank unmixing frame work can address these issues.

This paper is organized as follows. In section 2 deals with different unmixing methods. Paper is concluded in Section 3.

II. DIFFERENT UNMIXING METHODS

In this section, we review different unmixing algorithms, introducing LMM-based unmixing models, fully constrained least squares unmixing (FCLSU) [17], partial constrained least squares unmixing (PCLSU) [8], ELMM, PLMM and low rank-based approach using tensor [18].

Imaging spectrometers is used to measure electromagnetic energy scattered in hundreds or thousands of spectral bands with higher spectral resolution. Higher spectral resolution enables material identification and provide accurate information of material via hyperspectral image analysis, which improve different applications scenarios, unable for classical spectroscopic analysis that require identification of materials. Unmixing is the process of estimating the endmembers, and their abundances at each pixel. The information of the ground surface can be described by a three-dimensional structure, referred to as a data cube. Mixtures of the spectral signatures of the endmembers present in the scene is called hyperspectral vectors. Linear spectral mixture is the linear combination of the endmember present in the scene and the analysis aims at estimating the number of endmembers, their spectral signatures.

Variable illumination and environmental, atmospheric, and temporal conditions cause spectral variations within hyper spectral imagery. By ignoring these variations, errors are introduced in the unmixing process and these errors propagated throughout unmixing process. To develop accurate spectral unmixing and estimate spectral variabilities [19],[20], a number of approaches that account for spectral variability have been developed.

A lot of algorithms like Hyperspectral Signal Subspace Estimator (HySime) [21], Vertex Component Analysis (VCA) [22] N-FINDER [23] were introduced for hyperspectral unmixing. HySime for signal subspace identification, VCA for endmember extraction.

A. LMM

It is a simplest model, fast unmixing strategy. In linear mixing model (LMM) [24],[8] each observed spectrum in each pixel of a given image is assumed to resulting from the linear combination of endmember spectrum.

LetY= $[y_1, \ldots\ y_i, \ldots\ y_N] \in R_{D\times N}$ be an unfolded HSI with *D* bands and *N* pixels, and A = $[a_1, \ldots, a_p] \in R_{D\times P}$ be the endmembers with the size of $D \times P$. X =$[x_1, \ldots, x_i, \ldots, x_N] \in R_{P\times N}$ is denoted as abundance maps, whose each column vector stands for the fractional

abundance at each pixel R= $[r_1, \ldots, r_i \ldots, r_N] \in R_{D\times N}$ is the residual (e.g. noise, modelling errors and others) in the form of matrix. Linear combination of endmember spectra, resulting in the LMM can be represented as:

$$Y = Ax_i + r_i \quad (1)$$

where x_i should be non-negative in order to meet the physical constraints in reality. Moreover, the fractional abundance x_i, represents the proportions occupied by the different endmembers. This means x_i should be also satisfy sum-to-one constraint. Therefore, Eq. (1) with the necessary constraints is expressed as,

$$Y = Ax_i + r_i, \text{ s.t. } A\geq 0,\ x_i \geq 0,\ \sum_{i=1}^{N} x_i = 1; \quad (2)$$

Collecting all pixels in this model, a compact matrix form of Eq. (2) can be written as,

$$Y = AX + R, \text{ s.t. } A\geq 0,\ X \geq 0,\ \sum_{i=1}^{N} X = 1 \quad (3)$$

The LMM assumes that the pure material endmembers are fixed for all pixels $r_{n,}n = 1$, …., N, in the HSI. Spectral variability is not considered in LMM.

.

1)FCLSU: In practice, the endmembers (A) can be pre extracted from the given scene using vertex component analysis (VCA) [22]. This renders us to more effectively and conveniently estimate the abundance maps (X) by degrading the Eq. (3) to least-square problem, leading to FCLSU [17],

$$min_X \{\frac{1}{2}\|Y - AX\|_F^2, X \geq 0 \ \sum_{i=1}^{N} X = 1 \quad (4)$$

In the presence of spectral variability, FCLSU yields a poor performance. It mainly derives from the strong sum-to-constraint. A common way to solve this issue is to abundance fractions sum to less or larger than one or to consider a part of full constraints.

2) PCLSU: PCLSU can be formulated by solving

$$min_X \{\frac{1}{2}\|Y - AX\|_F^2, X \geq 0 \quad (5)$$

The estimated variable X in Eq. (5) might be any scales, owing to a badly-conditioned observed matrix Y. To alleviate the effects of the ill-posed problem, meaningfully physical assumptions have to be added in the form of regularization.

B. ELMM

Extended linear mixing model (ELMM) [13],[14] Effectively model changes in the observed spectrum due to illumination. ELMM aims to modeling the principle spectral variability (scaling factors) to allow a pixel-wise variation at each endmember, observed pixel can be represented as,

$$Y = Ax_iS_i + r_i \quad (6)$$

where $S_i \in R_{P\times P}$ is a diagonal matrix with the nonnegative constraint ($S_i \geq 0$). A matrix form of Eq. (6) can be repented as

$$Y = A\ (S \odot X) + R \quad (7)$$

here $S_i \in R_{P\times N}$ is a full matrix collecting the scaling factors from all pixels whose i_{th} column is S_i. The operator $\odot$ is denoted as the Schur-Hadamard (term wise) product. 1)*SPCLSU:* Prior to ELMM, SPCLSU is used to find the scaling factor [20] in which endmembers are reasonably assumed by sharing a same scale.The scaling factors are changed with topography. SPCLSU actually conducts a PCLSU in the beginning stage, and then normalizes the abundance maps to meet constrain of abundance that is sum-to-one. This is a simple but effective strategy, which is also involved in proposed method. Modelling capability of ELMM is limited.

C. PLMM

PLMM is a perturbated linear mixing model in which attempts to describe the spectral variability as an additive perturbation information. Both the pixel-wise and the corresponding matrix form of PLMM[15] can be expressed respectively

$$y_i = (A + \Delta_i)x_i + r_i \quad (8)$$

and

$$\Delta = [\Delta_1 x_i \ |\ldots\ |\Delta_i x_i \ |\ldots\ |\Delta_N x_N]$$

$$Y = AX + [\Delta_1 x_i \ |\ldots\ |\Delta_i x_i \ |\ldots\ |\Delta_N x_N] + R \quad (9)$$

where Δ is denotes the perturbation information of the endmembers.

1. Problem Formulation

PLMM and constraints can be combined to formulate a constrained optimization problem. An appropriate cost function is required to estimate the parameters M, A and dM. Signal is corrupted by a zero-mean white Gaussian noiseand data fitting term definedas the Frobenius norm of the difference between the acquisitions Y and the reconstructed data MA+Δ. Since the problem is ill-posed, additional penalization terms are needed for optimization. Penalization functions are $\Phi, \psi, and\ \Upsilon$. The optimization problem is expressed as,

$$(M^*, dM^*, A^*) \epsilon \arg\min_{M,A,dM} \{J(M, A, dM) s.t\} \quad (10)$$

with

$$J(M, A, dM) = \frac{1}{2} \|Y - MX - \Delta\|_F^2 + \alpha\, \Phi(A) + \beta\psi(M) + \gamma\, \Upsilon(dM) \quad (11)$$

where the penalization parameters α, β,γ control the trade-off between the data fitting term $\frac{1}{2}\|Y - MX - \Delta\|_F^2$and the penalties $\Phi(A)$, $\psi(M)$, and $\Upsilon(dM)$. In addition,here we assume that the penalization functions are separable, leading to the equations,

$$\Phi(A) = \sum_{n=1}^{N} \Phi(a_n) \quad (12)$$

$$\psi(M) = \sum_{l=1}^{L} \psi(m_l) \quad (13)$$

$$\Upsilon(dM) = \sum_{n=1}^{N} \upsilon(dM_n) \quad (14)$$

where $m_l$denotes the l throw of M and Φ, ψ and υ are non-negative differentiable convex functions. Due to the presents of large perturbation information PLMM is difficult to solve.

D. HySim

Hyperspectral Signal Subspace Estimator (HySime) is approach based on a mean squared error (MSE). It used to determine the signal subspace in hyperspectral imagery. HySime[21] is on eigen decomposition method; it estimates both signal and noise correlations matrices, then it considers the subset of eigenvalues which best represents the signal subspace in the least square error sense. This method has been optimized to reduce the computational complexity. Signal subspace identification is the major step in many hyperspectral processing applications such as target detection, change detection, classification, and unmixing. The identification of this subspace enables many advantages in unmixing algorithm, these includeacorrect dimensionalityreduction, improve the algorithm performance and complexity and in data storage. In a hyperspectral image each pixel y can be represented as,

$$y = x + n \quad (14)$$

where x and n are denotes the signaland additive noise, respectively.

1)Noise Estimation Noise estimation: Follow a multiple regression theory-based approach. The high correlation is present between neighboring spectral bands. The main reason for good performance of the multiple regression theory in hyperspectral applications is the high correlation. Let Y denote an L×N matrix, N denotes the spectral observed vectors and L is the size. Define the matrix $Z = V^T$T and the N ×1vector $z_i = [Z]_{:,i}$,where$[Z]_{:,i}$ stands for the ith column of Z and the N ×(L−1) matrix $Z_{\partial i}$ =[z_1,...,z_{i-1},z_{i+1},...,z_L]. Assume that z_i is explained by a linear combination of the remaining L−1 bands. Formally, this consists in writing,

$$z_i = Z_{\partial i}\, \beta_i + \xi_i \quad (15)$$

where $Z_{\partial i}$ is the explanatory data matrix, β_i is the regression vector of size (L−1) ×1, and ξ_i is the modeling error vector of size N ×1. For each i ∈{ 1,...,L}, the least squares estimator of the regression vector β_i is given by

$$\beta_i = (Z_{\partial i}^T\ Z_{\partial i})^{-1} Z_{\partial i}^T z_i \quad (16)$$

The noise is estimated by

$$\xi_I = z_i - Z_{\partial i}\beta_I \quad (17)$$

*2) Signal Subspace Estimation :*The signal subspace estimation is core structure of the proposed method. The first step, which is based on the noise estimation procedure

henceidentifies a set of orthogonal directions, of which an unknown subset spans the signal subspace. By seeking the minimum MSE between x, the original signal, and a noisy projection of it obtained from the vector y = x+u is usedto determined the subsets. We assume that u~N(0,Ru), i.e.,the noise is zero-mean Gaussian distributed with the covariance matrix Ru. Let the eigen decomposition of the signal sample correlation matrix R_x =[x_1,...,x_N][[x_1,...,x_N]^T/N be written as

$$\text{Rx} = E\Sigma E^T \quad (18)$$

E. N-FINDE

N-finder algorithm (N-FINDR)[23] has been widely used in endmember extraction. Several issues need to be addressed when implementing this algorithm.Computational complexity resulting from an exhaustive search, determination of endmembers, required for N-FINDR to generate,requirement of dimensionality reduction, and probably the most critical issue is its use of random initial endmembers which results in inconsistent final endmember selection and results are not reproducible are some disadvantages of N-FINDR algorithm. These disadvantages are overcome by implement the N-FINDR as a random algorithm, called random N-FINDR (RN-FINDR).

N-FINDR Steps

1. Preprocessing:

a) Let p denote the number of endmembers.

b) Apply a DR transform such as MNF to reduce the data dimensionality from L to p whereL is the total number of spectral bands.

2. Exhaustive search:

For an arbitrary set of p data sample vectors form $e_1, e_2, e_3 \dots, e_p$ a p vertex simplex specified by S($e_1, e_2, e_3 \dots, e_p$)and define its volume V($e_1, e_2, e_3 \dots, e_p$) by,

$$\text{V}(e_1, e_2, e_3 \dots, e_p) = \frac{|det\left[e_1^{\,1}\, e_2^{\,1 \dots 1}\, e_p\right]|}{(p-1)} \quad (20)$$

Find a set of data sample vectors in the data, denoted $\{e_1^*, e_2^*, e_3^* \dots, e_p^*\}$by , that form a p vertex simplex to yield the maximum value of (20), i.e.,

$$\{e_1^*, e_2^*, e_3^* \dots, e_p^*\} = arg\{\max_{e_1, e_2, e_3 \dots, e_p} \text{V}(e_1, e_2, e_3 \dots, e_p)\} \quad (21)$$

The set of $\{e_1^*, e_2^*, e_3^* \dots, e_p^*\}$ is the desired set of endmembers needed to be found. To complete the above exhaustive search in this step there are $\binom{N}{p} = \frac{N!}{(p!(n-p!))p!}$vertex simplexes needed to be compared based on the criterion specified. Spectral variability is not considered using N-FINDER and is less accurate using real data.

F. Vertex Component Analysis(VCA)

VCA is a fast algorithm to unmix hyperspectral data. It extracts endmembers using two facts:

(i) The endmembers are represented as a vertex of a simplex.

(ii) The transformation of a simplex is also a simplex.

VCA algorithm is having computational complexity between one and two orders of magnitude lower than the best available method.

InVCA [22] algorithm, is done using a subspace contain initial endmembers. The algorithm iteratively projects data onto a direction orthogonal to this subspace. The new endmember signature identified corresponds to the extreme of the projection. Fig. 4 shows the VCA algorithm applied to the simplex defined by the mixture of two endmembers. Which shows the two iteration of VCA algorithm. The extreme of the projection is selected as endmember.The number of iterations is same as the number of endmembers in data.

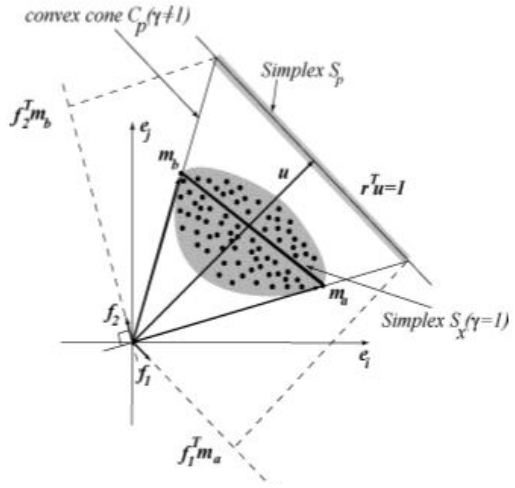

Fig. 4.Plot of mixtures of the three endmembers

The drawback of VCA is that, accuracy is low and does not contain all the data information's in the image.

G. Nonnegative Matrix Factorization (NMF)

Nonnegative matrix factorization (NMF)[16] ensures nonnegativity and no assumption for the presence of pure pixels. By introducing two constraints, namely, abundance separation and smoothness, into the algorithmfor optimization. NMF decomposes a set of hyperspectral data into two nonnegative matrices and finds "basis vectors". Here the original data are approximated through linear combination. Given the observation matrix R ∈ L×N and a positive number P<min(L, N), the objective of NMF is to find two matrices M and S with all elements being nonnegative and R ≈ MS holding. Problem is to formulate as,

$$J(M,S)=\|R-MS\|=\sum_{I,J}(R_{ij}-(MS)_{ij}) \quad (22)$$

The symbol "‖·‖" represents the Frobenius norm.

Augment R and M are as follows

$$M_A \leftarrow \begin{bmatrix} M \\ \delta 1^T \end{bmatrix} \quad (23)$$

$$R_A \leftarrow \begin{bmatrix} R \\ \delta 1^T \end{bmatrix} \quad (24)$$

After the initialization for M is finished, the initial S is generated by the equation,

$$S=(M^T M)^{-1}-M^T R \quad (25)$$

This method consider same noise level present in all bands, soit is fail to find reliable endmember and abundances. Spectral correlation is not considered.

H. Low-Rank Tensor Modelling

This method model spectral variability and spectral correlation usingtensor-based [25] strategies. Low rank decompositions of hyperspectral images areintroducing low-dimensional structures [18],[26] on the solutions of unmixing problems.The mixing model, combined with spatial regularization over the abundance and endmember estimations [27] is used to address the spectral variability [19] in the unmixing process.

Assuming that endmember matrix A has a low-rank representation as K_A, and abundance matrix M has a low-rankK_M.The global cost functional for the unmixing problem can be expressed as,

$$J(A,M)=\frac{1}{2}\sum_{n1=1}^{N1}\sum_{n2-1}^{N2}\left\|R_{n1,n2}-M_{n1,n2},:,A_{n1,n2}\right\| \quad (26)$$

s. t. rank $(M) = K_M, M \geq 0$,rank$(A) = K_A, A \geq 0,$

$$A \text{ x } 11_R = 1_{N1 \text{ x } N2}$$

By introducing new regularization terms controlled by two low-rank tensors $Q \in R^{N1XN2\,XR}$ and $P \epsilon^{N1XN2\,XLXR}$ to impose non-strict constraints on K_A and K_M. The λ_A, $\lambda_M \epsilon R^+$ are the two constraints introduced controlled the strictness of the low-rank constraint [18]. Then cost function is given by

$$J(A,M,P,Q) = \frac{\arg\, min}{A,M,P,Q}\frac{1}{2}\sum_{n1=1}^{N1}\sum_{n2-1}^{N2}\left\|R_{n1,n2} - Mn1,\ n2,\ :,\ :,An1,\ n2\right\|_F^2 + \lambda M2M-P\|_F^2 + \frac{\lambda_A}{2}\|A-Q\|_F^2$$

s. t. $M \geq 0$, $A \geq 0$, A x $^1 1_R = 1_{N1X\,N2}$ (27)

with rank (P) = K_M and rank(Q) = K_A.

Spectral correlation and low rank decompositions of hyperspectral images are considered using tensor based[28],[29] approach.Low-dimensional structures is implemented based on tensor.Which is asolution of standard and multitemporal unmixing problems. It hassuperior accuracy when compared with state-of-the-art unmixing algorithms.

III. CONCLUSION

This Paper is motivated by the fact that to study different unmixing methods. LMM is a simplest model used in unmixing. ELMM can

address the spectral variability. VCA, N-FINDR and HySime are used to estimate the endmembers and subspace identification with minimum error. The spectral signature in the original hyperspectral space inevitably suffers from largely and diversely spectral variabilities. Spectral correlation is also not considering in traditional hyperspectral analysis. To address this issue, implement a low rank tensor based unmixing method.

REFERENCES

[1] D. Hong, N. Yokoya, and X. Zhu, "Learning a robust local manifold representation for hyperspectral dimensionality reduction," IEEE J. Sel. Topics Appl. Earth Observ. Remote Sens., vol. 10, no. 6, pp. 2960–2975, Jul. 2017.

[2] D. Hong, N. Yokoya, J. Xu, and X. Zhu, "Joint & progressive learning from high-dimensional data for multi-label classification," in Proc. Eur. Conf. Comput. Vis., 2018, pp. 469–484.

[3] M. Veganzones, G. Tochon, M. Dalla-Mura, A. Plaza, and J. Chanussot, "Hyperspectral image segmentation using a new spectral unmixing-based binary partition tree representation," IEEE Trans. Image Process., vol.23, no. 8, pp. 3574–3589, Aug. 2014.

[4] T. Matsuki, N. Yokoya, and A. Iwasaki, "Hyperspectral tree species classification of Japanese complex mixed forest with the aid of lidar data," IEEE J. Sel. Topics Appl. Earth Observ. Remote Sens., vol. 8, no. 5, pp. 2177–2187, Apr. 2015.

[5] Z. Wang, R. Zhu, K. Fukui, and J. Xue, "Matched shrunken cone detector (MSCD): Bayesian derivations and case studies for hyperspectral target detection," IEEE Trans. Image Process., vol. 26, no. 11, pp. 5447–5461, Aug. 2017.

[6] L. I. Rudin, S. Osher, and E. Fatemi, "Nonlinear total variation based noise removal algorithms," Phys. D Nonlinear Phenom., vol. 60, no. 1,pp. 259–268, 1992.

[7] R. Heylen, M. Parente, and P. Gader, "A review of nonlinear hyperspectral unmixing methods," *IEEE J. Sel. Topics Appl. Earth Observ. Remote Sens.*, vol. 7, no. 6, pp. 1844–1868, Jun. 2014.

[8] J. M. Bioucas-Dias et al., "Hyperspectral unmixing overview: Geometrical, statistical, and sparse regression-based approaches," IEEE J. Sel. Topics Appl. Earth Observ. Remote Sens., vol. 5, no. 2, pp. 354–379, Feb. 2012.

[9] D. A. Roberts, M. Gardner, R. Church, S. Ustin, G.Scheer, and R. O. Green, "Mapping chaparral in the Santa Monica mountains using multiple endmember spectral mixture models," Remote Sens. Environ., vol. 65, no. 3, pp. 267–279, 1998.

[10] C. Yang, J. H. Everitt, Q. Du, B. Luo, and J. Chanussot,"Using high resolution airborne and satellite imagery to assess crop growth and yield variability for precision agriculture," Proc. IEEE, vol.101, no.3, pp.582– 592,Jul. 2013.

[11] J. Chi and M. M. Crawford, "Spectral unmixing-based crop residue estimation using hyperspectral remote sensing data: A case study at Purdue University," *IEEE J. Sel. Topics Appl. Earth Observ. Remote Sens.*, vol. 7, no. 6, pp. 2531–2539, Jun. 2014.

[12] Q. Qu, N. M. Nasrabadi, and T. D. Tran, "Abundance estimation for bilinear mixture models via joint sparse and low-rank representation," *IEEE Trans. Geosci. Remote Sens.*, vol. 52, no. 7, pp. 4404–4423, Jul. 2014.

[13] M.A. Veganzonesetal.,"A new extended linear mixing model to address spectral variability," in Proc.IEEE Workshop Hyperspectral Image Signal Process., Evol. Remote Sens., 2014, pp. 1–5.

[14] L. Drumetz, M. A. Veganzones, S. Henrot, R. Phlypo, J. Chanussot, and Jutten, "Blind hyperspectral unmixing using an extended linear mixing model to address spectral variability," *IEEE Trans. Image Process.*, vol. 25, no. 8, pp. 3890–3905, Aug. 2016.

[15] P. A. Thouvenin, N. Dobigeon, and J. Y. Tourneret, "Hyperspectral unmixing with spectral variability using a perturbed linear mixing model," IEEE Trans. Signal Process., vol. 64, no. 2, pp. 525–538, Jun. 2016.

[16] X. Liu, W. Xia, B. Wang, and L. Zhang, "An approach based on constrained nonnegative matrix factorization to unmix hyperspectral data," IEEETrans. Geosci. RemoteSens., vol.49,no.2,pp.757–772,Feb.2011.

[17] D. C. Heinz and C. I. Chang, "Fully constrained least squares linear spectral mixture analysis method for material quantification in hyperspectral imagery," *IEEE Trans. Geosci. Remote Sens.*, vol. 39, no. 3, pp. 529–545, Mar. 2001.

[18] Tales Imbiriba and Ricardo Augusto Borsoi "Low-Rank Tensor Modeling for Hyperspectral Unmixing Accounting for Spectral Variability" IEEE arXiv:1811.02413v1 Nov.2018.

[19] A. Zare and K. Ho, "Endmember variability in hyperspectral analysis: Addressing spectral variability during spectral unmixing," IEEE Signal Process. Mag., vol. 31, no. 1, pp. 95–104, Dec. 2014.

[20] J. M. Bioucas-Dias and J. M. P. Nascimento, "Hyperspectral subspace identification," *IEEE Trans. Geosci. Remote Sens.*, vol. 46, no. 8, pp. 2435–2445, Jul. 2008.

[21] J. M. P. Nascimento and J. M. Bioucas-Dias, "Vertex component analysis: A fast algorithm to unmix hyperspectral data," *IEEE Trans. Geosci.Remote Sens.*, vol. 43, no. 4, pp. 898–910, Apr. 2005.

[22] Chein-I Chang, Chao-Cheng Wu, and Ching-Tsorng Tsai:" N-FINDER Endmember Extraction Algorithms for Hyperspectral Imagery,"*IEEE trans. Image Processing*, vol. 20, no. 3, Mar. 2011

[23] J. M. Bioucas-Dias, ``A variable splitting augmented lagrangian approach to linear spectral unmixing," in *Proc. 1st Workshop Hyperspectral Image Signal Process., Evol. Remote Sens.*, Aug. 2009, pp. 1_4.

[24] H. Zhang,W. He, L. Zhang, H. Shen, and Q. Yuan, "Hyperspectral image restoration using low-rank matrix recovery," *IEEE Trans. Geosci. Remote Sens.*, vol. 52, no. 8, pp. 1–15, Aug. 2014.

[25] M. A. Veganzones, J. E. Cohen, R. C. Farias, J. Chanussot, and P. Comon, "Nonnegative tensor cp decomposition of hyperspectral data," IEEE Transactions on Geoscience and Remote Sensing, vol. 54, no. 5, pp. 2577–2588, 2016.

[26] T. Imbiriba, R. A. Borsoi, and J. C. M. Bermudez, "A low-rank tensor regularization strategy for hyperspectral unmixing," IEEE Statistical Signal Processing Workshop, pp. 373 – 377, 2018.

[27] L. De Lathauwer, B. De Moor, and J. Vandewalle, "A multilinear singular value decomposition," SIAM journal on Matrix Analysis and Applications, vol. 21, no. 4, pp. 1253–1278, 2000.

[28] A. Cichocki, D. Mandic, L. De Lathauwer, G. Zhou, Q. Zhao, C. Caiafa, and H. A. Phan, "Tensor decompositions for signal processing applications: From two-way to multiway component analysis," IEEE Signal Processing Magazine, vol. 32, no. 2, pp. 145–163, 2015.

[29] J. Hastad, "Tensor rank is np-complete," ˚ Journal of Algorithms, vol. 11, no. 4, pp. 644–654, 1990.